

Article

Wind Resource Assessment and Economic Viability of Conventional and Unconventional Small Wind Turbines: A Case Study of Maryland †

Navid Goudarzi ¹, Kasra Mohammadi ², Alexandra St. Pé ³, Ruben Delgado ⁴ and Weidong Zhu ^{5,*}

¹ Department of Mechanical Engineering, University of Maryland, College Park, MD 20742, USA; navid1@umd.edu

² Department of Chemical Engineering, University of Utah, Salt Lake City, UT 84112, USA; kasra.mohammadi@utah.edu

³ Department of Geography and Environmental Systems, University of Maryland, Baltimore County, Baltimore, MD 21250, USA; alexstpe@gmail.com

⁴ Joint Center for Earth Systems Technology, University of Maryland, Baltimore County, Baltimore, MD 21250, USA; delgado@umbc.edu

⁵ Department of Mechanical Engineering, University of Maryland, Baltimore County, Baltimore, MD 21250, USA

* Correspondence: wzhu@umbc.edu; Tel.: +1-410-455-3394

† This paper is an extended version of a paper published at the 4th Joint US-European Fluids Engineering Division Summer Meeting, Chicago, IL, USA, August 2014.

Received: 2 August 2020; Accepted: 25 October 2020; Published: 10 November 2020



Abstract: Annual mean wind speed distribution models for power generation based on regional wind resource maps are limited by spatial and temporal resolutions. These models, in general, do not consider the impact of local terrain and atmospheric circulations. In this study, long-term five-year wind data at three sites on the North, East, and West of the Baltimore metropolitan area, Maryland, USA are statistically analyzed. The Weibull probability density function was defined based on the observatory data. Despite seasonal and spatial variability in the wind resource, the annual mean wind speed for all sites is around 3 m/s, suggesting the region is not suitable for large-scale power generation. However, it does display a wind power capacity that might allow for non-grid connected small-scale wind turbine applications. Technical and economic performance evaluations of more than 150 conventional small-scale wind turbines showed that an annual capacity factor and electricity production of 11% and 1990 kWh, respectively, are achievable. It results in a payback period of 13 years. Government incentives can improve the economic feasibility and attractiveness of investments in small wind turbines. To reduce the payback period lower than 10 years, modern/unconventional wind harvesting technologies are found to be an appealing option in this region. Key contributions of this work are (1) highlighting the need for studying the urban physics rather than just the regional wind resource maps for wind development projects in the build-environment, (2) illustrating the implementation of this approach in a real case study of Maryland, and (3) utilizing techno-economic data to determine suitable wind harnessing solutions for the studied sites.

Keywords: wind resource assessment; distributed generation; urban physics; conventional and unconventional wind harvesting machines; feasibility; atmospheric variation; Maryland

1. Introduction

Built-environment wind turbine projects and wind innovations for rural economic development to fully integrate distributed wind R&D innovations to enhance resilience and reliability are still

developing. They are relatively less mature than the utility-scale wind or conventional ground-based distributed wind sector. Conducting a rigorous due diligence and devoting time to planning and testing before deployment increase positive outcomes of these projects. The goal of this paper is to study the impact of local terrain and atmospheric conditions to reduce risk and develop an empirical basis for cost and performance towards pursuing the development of wind harnessing solutions in areas with similar characteristics. The key research questions pursued in this paper include (1) how wind resource assessment analyses based on local and atmospheric circulation impacts are different from regional wind resource maps. (2) If the wind resource is not strong enough for large-scale power generation, would it be possible to leverage it for small-scale distributed power generation applications? (3) What are limitations and future steps towards reducing the payback period for making the application of small wind turbine solutions economic?

In this paper, the regional climate of Baltimore is first studied to provide context for the meteorological drivers impacting local wind power potential. Next, five years (2009–2013) of wind data collected throughout the Baltimore City megalopolitan area are analyzed to better understand the spatial and seasonal variability of residential-scale wind resource potential. Statistical analyses are carried out using collected wind data to determine the wind resource potential at the University of Maryland, Baltimore County (UMBC), Essex, and Padonia sites considering the climatological characteristics of the studied sites. Finally, in order to implement the results of the first part of the work, a number of small wind turbines based on the determined wind characteristics of the sites are selected. The economic evaluations of such distributed wind energy systems including conventional and modern (unconventional) small-scale wind turbines are evaluated and discussed. Finally, the conclusion summarizes key observations, limitations, and the application of this approach in areas with similar characteristics.

2. Literature Review

The world's electricity generation from wind and solar will be increased from 25% in 2017 to 85% by 2050 [1]. The USA's consumption of petroleum, natural gas, and coal constituted 80% of the total annual primary energy consumption in 2018 [2]. While the total energy consumption utilized by renewables in the USA was 19% in 2019 [2], the long-term plan is set to increase it up to 30% in 2030 [3]. As one of the cleanest, readily available, and environmental friendly renewable energy sources, wind energy has drawn more attention on the market and the wind development has had a rapid growth from 16 GW in 2007 to more than 74 GW in 2015 in the USA [4]. The average global annual growth in the total installed wind power capacity in the last ten years was over 25% per year [4]. The worldwide cumulative installed wind power capacity was 198 GW in 2010, and it passed 600 GW in 2020 [5,6]. There are novel solutions such as high-temperature superconducting generators, novel horizontal/vertical axis wind turbine designs, and unconventional configurations to address the implementation of wind harnessing in low-wind speed areas [4,7–13].

A thorough understanding of the site wind characteristics is the key in designing turbines that meet their optimum operation, reducing financial risks, and gaining investors' confidence. Statistical analysis of wind speed measurements is often used to evaluate the wind energy potential for a certain region. A variety of probability density functions (PDFs) are used to describe and predict wind speed frequency distributions, such as Pearson, Chi-Square, Weibull, Rayleigh, and Johnson functions [14–18]. Due to more accurate results fitting a variety of wind speed data at varying geographical locations, the Weibull distribution function is the most commonly used PDF for the wind speed distribution modeling [15,19–21].

To assist with understanding the potential for residential wind energy projects throughout the United States, the National Renewable Energy Laboratory (NREL) developed a residential-scale wind power classification tool that provides model-derived annual averaged wind speed estimates, at 2 km spatial resolution, and 30 m above the ground [22]. Across Baltimore City, the model's output suggests the residential-scale wind resource potential is on the cusp of "good" quality ($\leq \sim 4.0$ m/s) [22].

However, less is known regarding the spatial and seasonal variability of the wind resource, an important variable to assess when considering the availability of the resource to match residential/commercial electricity demand cycles. For example, on an inter-annual time-scale, Maryland electricity consumption peaks during the spring and summer months; there is then high demand for cooling [22]. As residential electricity demand in Maryland is expected to increase by 8% by 2021 [23], an advanced understanding of the spatial and seasonal variability of the residential wind power potential across Baltimore City would be helpful for planning purposes, and is therefore addressed in this study.

More in-depth literature review related to the seasonal variability and inter-site variability is provided in Sections 4.1 and 4.2. In addition, the related literature on choosing wind harnessing solutions for the implementation of this methodology on the studied sites is provided in Section 7.

3. Data Collection

Wind speed and direction data were collected from 2009 to 2013 at meteorological towers located at UMBC (39.2543° N, 76.7098° W), the Maryland Department of the Environment's Padonia (39.4620° N, 76.6315° W), and Essex (39.3107° N, 76.4744° W) air quality monitoring stations [24]. To aid in the approximation of the power law extrapolation for matching Essex and Padonia wind statistical heights (i.e., 10 m) to that of UMBC (i.e., 30 m), 2012 Beltsville station (39.0554° N, 76.8785° W) wind data at approximately similar heights were also evaluated. Figure 1 illustrates the four sites' locations within the Baltimore City metropolitan area used in this analysis. Note that the Beltsville station measurements are for obtaining true values for the shear component α , rather than using a generic value; this is further explained in Section 5.



Figure 1. Locations of meteorological stations assessed in this study: UMBC, Padonia, Essex, and Beltsville.

The UMBC wind data are collected from an NRG #40 cup anemometer, sampled with a 30-min temporal resolution at the height of 30 m from the ground. The site is situated at ~53 m elevation from the sea level, and is located 9.3 km Southwest of Baltimore. Padonia and Essex wind data are

sampled using a Vaisala WXT520 anemometer with a temporal resolution of 10 min, at the height of 10 m from the ground, following the International Energy Agency Task 27. A reliable design that resists fatigue loads and resonance due to gust required by such a high-resolution and site-specific study. For consistency in the comparison of the wind resource potential for residential-scale wind assessment analysis, 10 m wind measurements at Padonia and Essex sites are extrapolated to 30 m using the industry standard power law technique. Typically, when measurements above the surface are unavailable, the power law's wind shear exponent α is assumed to be one-seventh (0.14), representing neutral atmospheric stability [25]. However, empirically determined α values may deviate from this value due to non-neutral atmospheric stability and local terrain effects [26]. Therefore, to improve the accuracy of the power law extrapolation of 10 m to 30 m, wind speeds at Essex and Padonia, empirically derived monthly α values between similar heights at Beltsville air quality station, in Beltsville, MD are utilized over standard values. Beltsville location was chosen as the closest location with available 30 m wind speed measurements, approximately 45 km and 50 km Southwest of Essex and Padonia, respectively. In addition, the terrain of Beltsville is similar to those of Essex and Padonia, in that the site is surrounded by open space and few trees.

4. A Brief Review of Baltimore City Climate

Understanding a region's site-specific climate is essential for wind projects and should be acknowledged in planning and policy decisions [27]. Maryland has a unique geography: Appalachian Mountains on the West and sloping coastal plains and the moderating influence of the Atlantic Ocean on the East. This results in observing large-scale and diverse weather patterns with significant changes by season and topography. An overview of seasonal synoptic and microscale metrological processes gives a better understanding of the wind energy potential across the Baltimore metropolitan area.

4.1. Seasonal Variability

The jet stream is a planetary-scale wind circulation and often governs the storm track of mid-latitude extratropical cyclones. This meandering ribbon of fast winds in the upper atmosphere is typically found at an altitude of 7–12 km above ground. In the Northern Hemisphere, the polar jet stream is the boundary between high-latitude cold and lower-latitude warm air. Natural climate factors cause seasonal changes in the polar jet stream's altitude, location, and intensity, thereby impacting Maryland's regional climate and wind energy potential. During Northern Hemisphere winter (December, January, and February (DJF) in Figure 2a), the surface temperature gradient between cold arctic and warmer tropical air over the USA and further South is strong, parking a strong polar jet stream near Maryland. Hence, active weather patterns, such as mid-latitude extratropical cyclones, traverse Maryland, bringing frequent, intense, and sustained wind regimes across Baltimore (e.g., cold fronts, coastal low pressure systems, Nor'easters, etc.). On the contrary, during Northern Hemisphere summer (June, July, and August (JJA) in Figure 2b), the surface temperature gradient over the USA weakens, causing the polar jet stream to retreat poleward toward stronger gradient regions, and warm air originating from the equator to expand North over the continental USA. The weakening of the temperature and pressure gradient over Maryland, coupled with the poleward shift of the jet stream and storm track over Baltimore, occurs contemporaneously with a strengthening of the semi-permanent Bermuda high-pressure system over the Atlantic Ocean. Therefore, during the summer season, generally weaker, anticyclonic, southwesterly wind speeds persist, and quiescent weather persists in Maryland and along the Eastern seaboard (Figure 2b) [28].

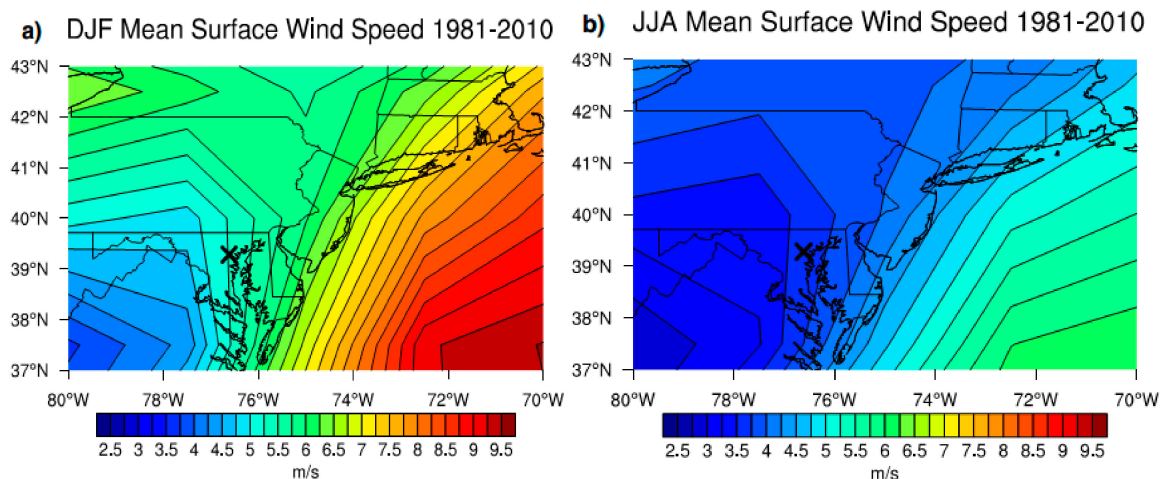


Figure 2. (a) Seasonal mean winter (DJF) and (b) summer (JJA) surface scalar wind speeds from National Centers for Environmental Prediction/National Center for Atmospheric Research (NCEP/NCAR) reanalysis data based on 1981–2010 climatology (crosshair represents Baltimore County, MD).

4.2. Inter-Site Variability

On a smaller temporal and spatial scale, landscape discontinuities can modify surface thermal fluxes [29] and surface wind characteristics [30]; they also play a critical role in wind climatology [31–35]. For example, differences between land surfaces can lead to thermally induced mesoscale circulations (~20–200 km), notably during relatively weak large-scale forcing during summer, in which temperature differences between land and adjacent water drive changes in atmospheric stability, thus development of land or sea breezes [36–41]. The development of the diurnal Chesapeake Bay breeze circulation at coastal locations in Maryland is well known [42–44]. Due to the daytime absorption of solar radiation, land becomes warmer than water, motivating a local pressure difference, thus a breeze from the bay inland. The effects of the daytime bay breeze are observed nearly daily in Essex during the summer season, in which calm/stagnant conditions and wind flow rates are recorded [42], thereby contributing to its seasonal wind resource potential.

Further, beyond mesoscale circulation systems, the influence of microscale topography and obstructions on site-specific wind regimes cannot be overlooked. For example, Padonia site in Baltimore City is above the Fall Line within Piedmont plateau. Alternatively, Essex lies below the Fall Line within a coastal plain, approximately 1 km from the shore of the Black River that feeds in to the Chesapeake Bay, while UMBC is juxtaposed to the Fall Line, and considered the most urban of the sites given its proximity to downtown Baltimore City (<10 km). Although a comprehensive analysis of the site-specific topographical impact on the surface wind speed is beyond the scope of this analysis, it is important to consider such small differences in landscape that may contribute to differences in the local wind resource potential.

5. Analysis Procedure

Wind speed extrapolation with the height. The UMBC wind data were measured at 30 m above the ground, but the Padonia and Essex wind data were measured at 10 m. Therefore, the power law is used to calculate the wind speed data at 30 m height for Essex and Padonia [45]. Given the seasonality of shear exponent values found, empirical monthly α values from Beltsville are substituted in the power law equation to extrapolate wind speeds to the 30 m height at Essex and Padonia (rather than using a single annual α value).

Probability density function. Statistical methods such as PDFs can be used to estimate the wind characteristics and wind potential at any site. In this study, the Weibull distribution function is used

due to its simplicity and favorable accuracy [46]. The probability function $f(u)$ of observing a wind speed using the Weibull distribution function is determined by [47]

$$f(u) = \frac{k}{c} \left(\frac{u}{c}\right)^{k-1} \exp\left(-\left(\frac{u}{c}\right)^k\right), \quad (k > 0, u > 0, c > 1), \quad (1)$$

where k and c are the Weibull shape and scale parameters. In an earlier work [48], the performance of six different methods for calculating Weibull distribution parameters are studied and compared: (1) graphical method (GP), (2) empirical method of Justus (EMJ), (3) empirical method of Lysen, (4) energy pattern factor (EPF), (5) maximum likelihood method (ML), and (6) modified maximum likelihood method (MML). A similar approach conducted here and it was found that the EMJ gives an accurate estimation. Since the focus of this work is on identifying solutions with a better payback period (PBP), readers are encouraged to read [48] for detailed analysis and comparison of these methods. Based on this method, the Weibull distribution parameters are defined by [13]

$$k = \left(\frac{\sigma}{\bar{u}}\right)^{-1.086} \quad (1 \leq k \leq 10), \quad (2)$$

$$c = \frac{\bar{u}}{\Gamma(1 + 1/k)}, \quad (3)$$

where \bar{u} is the mean wind speed, σ is the variance, and Γ is the gamma function. To assess the performance of the EMJ in the studied site, statistical indicators such as relative percentage error (RPE), mean absolute percentage error (MAPE), mean absolute bias error (MABE), root mean square error (RMSE), and relative root mean square error (RRMSE) are utilized:

$$RRMSE = \frac{RMSE}{\frac{1}{n} \sum_{i=1}^n P_{i,M}} \times 100 = \frac{\sqrt{\frac{1}{n} \sum_{i=1}^n (P_{i,W} - P_{i,M})^2}}{\frac{1}{n} \sum_{i=1}^n P_{i,M}} \times 100, \quad (4)$$

where $P_{i,W}$ is the i^{th} calculated wind power density using the Weibull distribution function, $P_{i,M}$ is its calculated wind power density using measured data, and n is the total number of observations. The average wind power and energy densities for a desired time duration, using the Weibull density function are calculated using Equations (5) and (6), respectively:

$$\bar{P}_w = \frac{1}{2} \rho A \int_0^{\infty} u_i^3 f(u) du = \frac{1}{2} \rho c^3 \Gamma\left(\frac{k+3}{k}\right) = \frac{\rho A \bar{u}^3 \Gamma(1 + 3/k)}{2[\Gamma(1 + 1/k)]^3}, \quad (5)$$

$$E = \left(\frac{1}{2} \rho A u^3 f(u)\right) D = \frac{1}{2} \rho A c^3 \Gamma\left(\frac{k+3}{k}\right) D. \quad (6)$$

6. Results and Discussion

6.1. Wind Patterns

The monthly mean wind speeds and wind directions as well as the Weibull distribution parameters, wind power, and energy density at three studied sites of UMBC, Padonia, and Essex are calculated based on five-year measured wind speed data. Figure 3 shows the monthly mean wind speed and its standard deviation as well as the wind direction at the 30 m height for UMBC, Padonia, and Essex, respectively. The monthly mean wind speed values are in the range of 2.30–3.56 m/s, 1.90–4.10 m/s, and 1.75–2.80 m/s, respectively. Wind speeds are higher at more urban sites (i.e., UMBC and Padonia), and weaker at the coastal site (i.e., Essex) where a climatologically persistent small-scale bay breeze circulation often promotes stagnant wind conditions (Section 4.2). Annual trends of wind speed distribution at each site are similar, reflecting seasonal fluctuations in the cold season storm track

(Section 4.1), in which monthly mean wind speed maximum and minimum values occur during winter and summer, respectively. Similarly, wind speed standard distributions reflect seasonal patterns of storm activity traversing the region, with the maximum variance found during winter and minimum values during summer. At UMBC, Padonia, and Essex, the monthly speed deviations range between 1–2 m/s, 1–3 m/s, 0.5–1.5 m/s, respectively. Padonia winds demonstrate the highest wind speed variance; it is likely due to local obstructions and proximity to a complex terrain (higher elevation). Similar to the wind speed results, the variance of the wind speed is also the lowest at Essex, which may also be influenced by the bay breeze circulation.

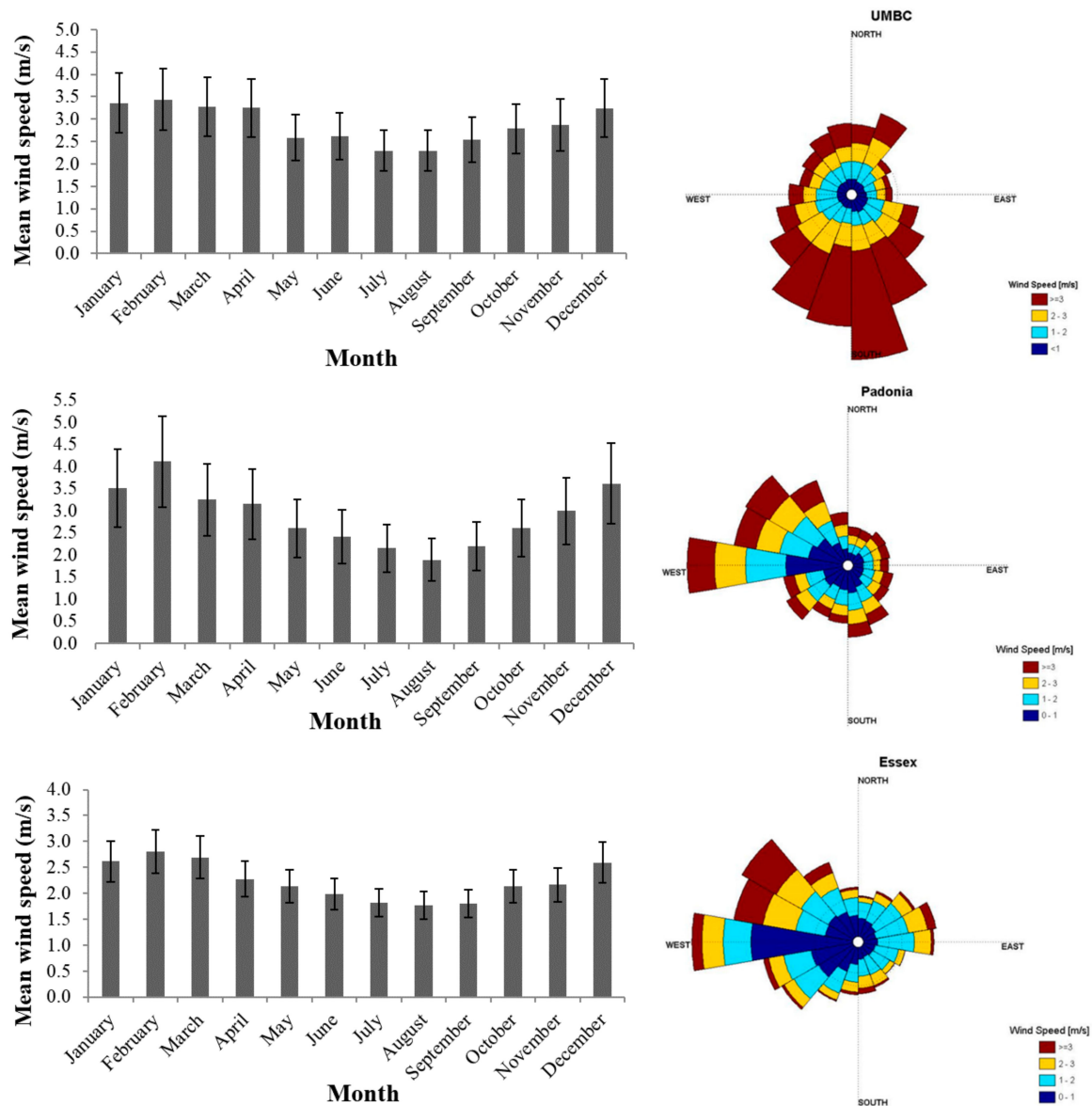


Figure 3. Five year averaged (left) monthly mean wind speeds and standard deviations at the 30 m height and (right) wind directions for UMBC (top), Padonia (middle), and Essex (bottom).

The most probable wind directions at different wind speed distributions for all three sites are illustrated by wind roses in Figure 3 [49]. The relationship between wind speed magnitude and direction varies by site, with higher speeds associated with Southerly, Northwesterly, and Westerly flow for UMBC, Padonia, and Essex, respectively. Wind speed and directional differences among sites

are likely related to the local topographical effects (Section 4.2), and are important to consider in more robust assessments of residential wind turbine designs and layouts.

6.2. Performance Evaluation of Weibull Parameter Estimation Methods

Using the EMJ approach in determining the Weibull distribution parameters, the statistical indicators are summarized in Table 1. For the RRMSE, the model accuracy is defined by: RRMSE < 10%, Excellent; 10% < RRMSE < 20%, Good; 20% < RRMSE < 30%, Fair; and RRMSE > 30%, Poor. UMBC and Padonia show an excellent accuracy in the predicted wind power density values and the Essex results are very close to the excellent level.

Table 1. Performance demonstration of the utilized EMJ method.

	UMBC	Padonia	Essex
RPE	2.3–10.5%	0.2–11%	3–11%
MAPE	7.62%	4.46%	8%
MABE	2.91 W/m ²	1.11 W/m ²	1.06 W/m ²
RMSE	3.19 W/m ²	2.48 W/m ²	1.30 W/m ²

Table 2 presents the main seasonal wind characteristics for studied sites, including average wind speed (\bar{u}), standard deviation (σ), k and c parameters, most probable wind speed (u_{mp}), and wind speed carrying the maximum energy ($u_{max, E}$); u_{mp} is the most frequent wind speed for a given wind probability distribution and $u_{max, E}$ is the wind speed which carries the maximum wind energy [15]. Higher k values indicate a higher peaked wind speed distribution. All three sites have relatively close ranges of k and c . The monthly k values change from 1.5 to 2.1, which shows a regular and uniform behavior at the studied sites. The monthly c values vary from 1.7 m/s to 3.8 m/s, which shows that the site is not very windy and is expected to have a lower wind power potential. The range of the annual c parameter in the studied sites is from 2.06 m/s to 3.57 m/s; it reflects the annual mean wind speed trend to be the highest at UMBC and the lowest at Essex, also consistent with general wind statistics (Section 4).

Table 2. Seasonal wind characteristics for studied sites.

Season	\bar{u} (m/s)	σ	k	c (m/s)	u_{mp} (m/s)	$u_{max, E}$ (m/s)	Power Density (W/m ²)	Energy Density (kWh/m ²)
UMBC								
Winter	3.35	2.09	1.68	3.75	2.17	6.01	53.79	38.38
Spring	3.04	1.71	1.86	3.40	2.26	5.03	35.43	25.84
Summer	2.40	1.30	1.95	2.69	1.86	3.86	16.22	11.95
Fall	2.73	1.51	1.92	3.06	2.20	5.35	24.84	18.48
Padonia								
Winter	3.145	1.978	1.663	3.522	2.007	5.699	36.684	30.446
Spring	2.446	1.517	1.679	2.740	1.599	4.370	17.556	13.655
Summer	1.923	1.131	1.783	2.154	1.354	3.291	7.557	5.814
Fall	2.613	1.756	1.526	2.927	1.463	5.059	34.100	25.142
Essex								
Winter	2.337	1.478	1.652	2.617	1.477	4.258	20.740	14.821
Spring	1.903	1.076	1.872	2.132	1.404	3.164	9.422	6.874
Summer	1.571	0.841	1.978	1.760	1.227	2.514	4.918	3.575
Fall	1.970	1.272	1.799	2.206	1.382	3.380	13.637	10.067

6.3. Wind Power and Energy Densities

The seasonal wind power density (P) and wind energy density (E) for all studied sites are presented in Table 2. UMBC has the highest monthly wind power and wind energy densities, and Essex has the lowest. In addition, the maximum and minimum values of wind power and wind energy densities are in February and August, respectively, for all three sites; this reflects the previously discussed seasonal climatology (i.e., winter versus summer) of the region (Section 4.1). To determine the minimum wind power density requirements of a site for developing wind harnessing technologies, several classifications are proposed in the literature [50–52]. In this work, the wind power classification proposed by Elliot and Schwartz [51,52] is used. Baltimore City is considered a poor site (class 1) for electricity generation using wind energy. As previously discussed, all sites demonstrate the greatest wind energy potential during the winter season, related to the regional climatology (Section 4).

7. Implications of the Study: Integrating Wind Energy Harvesting Technologies in the Built Environment

7.1. Conventional Wind Energy Systems

While small-scale wind turbines generally produce more expensive electricity than large-scale wind turbines, they can still be a reliable source of energy when sized properly and used at their optimum conditions. Besides the performance limitations, such as low mean wind speeds, high turbulence, and high aerodynamic noise levels, the initial cost per rated power and unit-cost per generated power per hour should be calculated to evaluate the performance of small-scale wind turbines.

Baltimore City, with a low annual mean wind speed, is a location where certain basic performance limitations for employing wind harnessing technologies apply. Christiner et al. [53] studied more than 80 rooftop horizontal axis wind turbines (HAWTs) and vertical axis wind turbines (VAWTs) for power generation in Boston, Massachusetts. The wind turbines have a cut-in speed range from 1.8 m/s to 3.2 m/s, and a rated speed range from 5.4 m/s to 14.75 m/s [54]. The wind assessment results for Baltimore City indicates wind speeds lower than 5 m/s throughout a year, i.e., the minimum designed rated speed for HAWTs and VAWTs. Hence, employing these types of wind turbines is not feasible for this site. There are a number of researchers whose research is focused on designing and characterizing small-scale wind energy turbines that operate at wind speeds lower than 5 m/s [55].

The performance of small-scaled HAWTs for low-wind speed applications is studied by a number of researchers [53–55]. HAWTs have higher energy production compared to other wind harnessing technologies; however, their performance will be strongly affected by gusts, turbulence, and large variations in mean wind speeds and wind directions. VAWTs have shown significant advantages over HAWTs in terms of having an omni-directional design, an expanded operational range, building integration, reliability, and overall cost. However, further studies are required to improve their rated power and efficiency, especially at lower wind speeds [56].

In this study, the potential of small-scale wind turbines is evaluated by analyzing the performance of three small-scale HAWTs with rated powers of 2.1 kW, 6 kW, and 10 kW (Travere 2.1, Proven WT 6000, and Aircon 10). The main specifications of these three wind turbines are presented in Table 3. These wind turbines were chosen among several available HAWTs because their rated speeds have a better match with wind speed characteristics of the examined stations. It should be noted that these analyses were done only for the UMBC station due to its higher wind energy potential.

Table 3. Main specifications of analyzed wind turbines [57].

Wind Turbine	Rated Power (kW)	Cut-in Speed (m/s)	Rated Speed (m/s)	Cut-Out Speed (m/s)	Rotor Diameter (m)
Travere 2.1	2.1	2.5	8	60	6
Proven WT 6000	6	2.5	12	none	5.5
Aircon 10	10	2.5	11	32	7.1

The capacity factor (CF) is defined as the ratio of the generated output power of a wind turbine to that at its rated power. It is a function of several parameters, including the location wind characteristics and wind turbine performance characteristics such as the cut-in speed, rated speed, and cut-out speed. The annual CF values are calculated for the selected wind turbines at the 30 m height above the ground. The CF for Travere 2.1, Proven WT 6000, and Aircon 10 wind turbines are 11%, 5%, and 7%, respectively. The Travere 2.1 kW wind turbine has the highest CF and the lowest rated speed (8 m/s). As noticed, due to its larger size, Aircon 10 produces the highest electricity per year, which is around 6058 kWh. Travere 2.1 and Proven WT 6000 can generate around 1990 kWh and 2600 kWh energy annually, respectively. However, the selection of the most appropriate turbine for the site is a function of both the power generated and cost of electricity.

To determine the economic feasibility of the selected wind turbines, PBP analysis was carried out [58,59]. For this analysis, the following main assumptions were made: (1) the average total cost of small wind turbines is \$3000/kW, (2) the average life time of selected wind turbines is 30 years, (3) the variable cost is \$0.005/kWh, (4) the nominal variable cost escalation rate is 2% per year, and (5) availability of wind turbines is 98%.

Currently, the average cost of electricity (COE) in Maryland is around \$0.14/kWh [59]. Hence, the generated power from wind turbines can be sold at this price or higher. Figure 4a illustrates the calculated values of PBP at different selling prices, changing from \$0.14/kWh to \$0.22/kWh for the selected wind turbines. The desired COE has a significant influence on the economic feasibility of wind turbines. As noticed and expected, PBP decreases substantially when electricity price increases to \$0.22/kWh. Hence, to achieve a lower PBP, the COE should be increased significantly. Among selected wind turbines, Travere 2.1 kW can have the lowest PBP range, changing from 19 years to 13 years when the electricity price increases from \$0.14/kWh to \$0.22/kWh, respectively.

Government incentives offered for small wind turbine projects would improve the wind turbines' economic feasibility, e.g., one of the most attractive incentives at the current time is the Federal Investment Tax Credit, which covers 30% of the total initial cost of the project [54]. Such incentives can improve the economic feasibility of small wind turbines at the UMBC site. In Figure 4b, the impact of incentive variation (changing from 0% to 30%) on the PBP for a COE of \$0.18/kWh is shown for Travere 2.1 kW. It is seen that incentives can substantially improve the economic feasibility of installing the Travere 2.1 kW wind turbine. By the 30% incentive, the PBP can be reduced from 15.7 years to 11.8 years. This makes installation of the Travere 2.1 kW wind turbine at the UMBC site more attractive despite the relatively low available wind energy potential at the site.

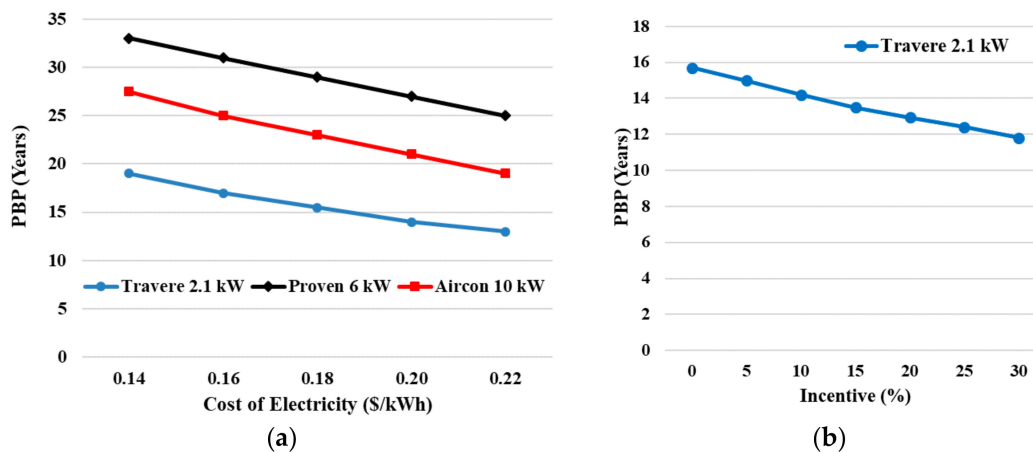


Figure 4. (a) Payback period (PBP) for different rates of selling electricity prices (\$/kWh). (b) Effect of incentives on the PBP at fixed selling electricity prices of \$0.18/kWh.

7.2. Unconventional/Modern Wind Energy Systems

Novel unconventional wind harnessing technologies can be another solution to common obstacles that lower turbine performance, such as low mean wind speeds, high turbulence, and high aerodynamic noise levels. Ducted turbines have been studied as an alternative to conventional roof-mounted wind turbines [56]. Figure 5a illustrates a schematic of a novel ducted turbine. Ducted turbines are protected from turbulent effects and offer much less aesthetic impacts compared to conventional turbines. Moreover, the location of the turbine inside the duct and the omni-directional feature reduces the wind speed/direction fluctuations. Since the turbine is inside the duct, a compromise on power performance to achieve low-aerodynamic noise radiations is not necessary; instead, a blade design with an optimum output power can be employed. The probability analysis on the five-year wind speed distribution at UMBC at 30 m above the ground has shown that this site experiences average wind speeds higher than 5 m/s on 40+ days of a year and average wind speeds higher than 10 m/s might occur a few days a year. A high-performance wind harnessing technology with a rated power less than 10 m/s can provide a cost-effective stand-alone solution, if one wants to generate electricity from wind at this site.

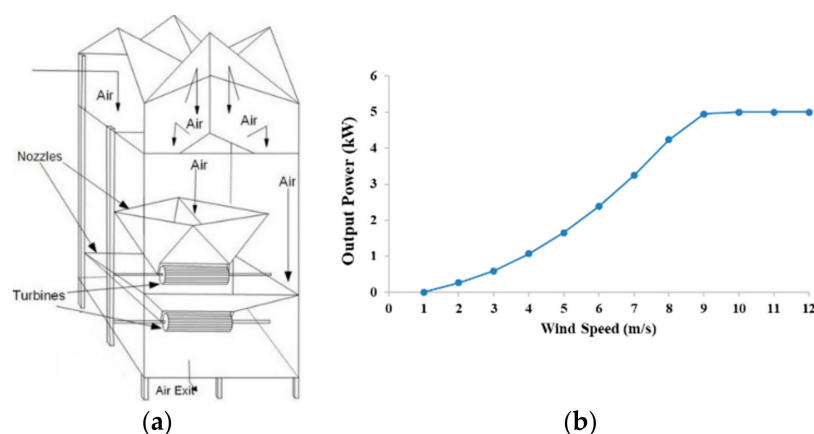


Figure 5. (a) Schematic of a ducted wind turbine. (b) A generic ducted turbine power curve.

Full-scale proven 5 kW unconventional ducted turbine specifications are used for conducting the PBP analysis. Figure 5b shows a generic power curve of a ducted turbine, obtained from conducting computational fluid dynamic analysis of the flow within a ducted turbine, similar to the one shown in Figure 5a, but with one nozzle and one turbine. It has a 1 m/s cut-in speed [60], and a 9 m/s rated speed. The total installed cost of the system is estimated to be \$15,000. Using the same site assumptions as

those used for conventional wind systems, the PBP for the cost of electricity varying from 0.14 \$/kwh to 0.22 \$/kwh, changes from 16 years to 10 years, respectively. Compared to Travers 2.1 kW with the PBP of 19 years to 13 years, the 5 kW unconventional ducted turbine confirms its economic benefit [11,61]. For a fixed cost of electricity of 0.18 \$/kwh and a 30% government incentive, the PBP can be reduced from 13 years to 10 years.

8. Conclusions

In this multidisciplinary study, the potential of wind power production in the Baltimore metropolitan area, Maryland, USA is studied, and the feasibility of installing wind energy systems is evaluated and discussed. The important findings can be summarized as follows:

- (a) There is a maximum 43% probability for having wind speeds larger than 3 m/s. Results are consistent with the NREL residential wind power classification. Spatial and seasonal variability among sites makes it suitable for non-grid connected electrical and mechanical applications.
- (b) The strongest and weakest wind power and energy density values were observed at UMBC, Padonia, and Essex sites, respectively. Higher wind speeds at UMBC compared to other sites could be related to its position above the Fall Line, along the Piedmont Plateau, while weaker winds in Essex are related to stagnation from the persistence of a local bay breeze circulation.
- (c) Among examined distributed wind energy solutions, including conventional HAWTs, an annual CF of 11% with an electricity production of 1990 kWh is feasible. Economic analysis showed that it has the lowest PBP, which changes from 19 years to 13 years when the electricity price increases from \$0.14/kWh to \$0.22/kWh, respectively. Government incentives improve the economic feasibility.
- (d) Employment of modern wind harvesting machines in Baltimore City, a low-wind speed region, supports extending the use of wind energy for power generation.
- (e) Limitations and future work: While significant work has been performed on optimizing performance parameters of turbines, more research on the impact of wind gust, turbulence intensity, ease of manufacturing, and cost on airfoil/rotor designs are required. In addition, both spatial and temporal metrological analysis from macroscale to building scales should be conducted to better understand the urban physics and pertinent parameters in optimizing wind harnessing technologies; these include employing both computational and experimental fluid dynamic analysis of a studied site.

Author Contributions: Conceptualization, N.G.; methodology, N.G., R.D., A.S.P., and K.M.; software, N.G. and K.M.; validation, N.G. and K.M.; formal analysis, N.G., K.M., and A.S.P.; data curation, N.G.; writing—original draft preparation, N.G., K.M., and A.S.P.; writing—review and editing, N.G. and W.Z.; supervision, W.Z.; project administration, W.Z. and R.D. All authors have read and agreed to the published version of the manuscript.

Funding: This research did not receive any specific grant from funding agencies in the public, commercial, or not-for-profit sectors.

Acknowledgments: The authors gratefully acknowledge the Howard University Beltsville Research Campus and Maryland Department of the Environment for providing meteorological data for Beltsville, and Padonia and Essex, respectively. We would also like to acknowledge Joseph Brodie from the Joint Center for Earth Systems Technology and Scott Rabenhorst from the Naval Research Laboratory for their support and insightful comments on the climatological review.

Conflicts of Interest: The authors declare no conflict of interest.

References

1. IRENA. *Global Energy Transformation: A Roadmap to 2050*; International Renewable Energy Agency: Abu Dhabi, UAE, 2018; ISBN 978-92-9260-059-4. Available online: <https://www.irena.org/publications/2018/Apr/Global-Energy-Transition-A-Roadmap-to-2050> (accessed on 15 July 2020).

2. US Department of Energy (DOE); Energy Information Administration (EIA). Annual Energy Outlook 2050. 2020. Available online: <https://www.eia.gov/outlooks/aeo/pdf/AEO2020%20Full%20Report.pdf> (accessed on 15 July 2020).
3. US Department of Energy (DOE). Wind Vision: A New Era for Wind Power in the United States. 2020. Available online: <http://energy.gov/eere/wind/wind-vision> (accessed on 15 July 2020).
4. Goudarzi, N.; Zhu, W.D. A review on the development of the wind turbine generators across the world. *Int. J. Dyn. Control* **2013**, *1*, 192–202. [[CrossRef](#)]
5. Lee, J.A.; Doubrawa, P.; Xue, L.; Newman, A.J.; Daxl, C.; Scott, G. Wind resource assessment for Alaska's offshore region: Validation of a 14-year high-resolution WRF data set. *Energies* **2019**, *12*, 2780. [[CrossRef](#)]
6. Dorrell, J.; Lee, K. The cost of wind: Negative economic effects of global wind energy development. *Energies* **2020**, *13*, 3667. [[CrossRef](#)]
7. Poore, R.; Lettenmaier, T. *Alternative Design Study Report: WindPACT Advanced Wind Turbine Drive Train Designs Study*; NREL/SR-500-33196; National Renewable Energy Laboratory (NREL): Golden, CO, USA, 2003.
8. Polinder, H.; Van Der Pijl, F.F.A.; De Vilder, G.-J.; Tavner, P.J. Comparison of Direct-Drive and Geared Generator Concepts for Wind Turbines. *IEEE Trans. Energy Convers.* **2006**, *21*, 725–733. [[CrossRef](#)]
9. Goudarzi, N.; Zhu, W.D. Offshore and onshore wind energy conversion: The potential of a novel multiple-generator drivetrain. *Key Eng. Mater.* **2013**, 569–570, 644–651. [[CrossRef](#)]
10. Mikhail, A.; Petch, D. Clipper Liberty series: Advanced low wind speed technology. Paper Presented in California Wind Energy Collaborative Forum, Davis, CA, USA, 14 December 2005.
11. Goudarzi, N.; Zhu, W.D.; Bahari, H. An assessment of the potential of a novel ducted turbine for harvesting wind power. *J. Intell. Mater. Syst. Struct.* **2014**, *26*, 1059–1070. [[CrossRef](#)]
12. Wu, J.; Wang, J.; Chi, D. Wind energy potential assessment for the site of Inner Mongolia in China. *Renew. Sustain. Energy Rev.* **2013**, *21*, 215–228. [[CrossRef](#)]
13. Goudarzi, N.; Zhu, W.D.; Delgado, R.; Pe, A. An assessment on the wind energy potential and possible solutions for power generation in Baltimore County in Maryland, USA. In Proceedings of the ASME 4th Joint US-European Fluid Engineering Division Summer Meeting, Chicago, IL, USA, 3–7 August 2014.
14. Keyhani, A.; Ghasemi-Varnamkhashti, M.; Khanali, M.; Abbaszadeh, R. An assessment of wind energy potential as a power generation source in the capital of Iran, Tehran. *Energy* **2010**, *35*, 188–201. [[CrossRef](#)]
15. Hamouda, Y.A. Wind energy in Egypt: Economic feasibility for Cairo. *Renew. Sustain. Energy Rev.* **2012**, *16*, 3312–3319. [[CrossRef](#)]
16. Zhou, J.Y.; Erdem, E.; Li, G.; Shi, J. Comprehensive evaluation of wind speed distribution models: A case study for North Dakota sites. *Energy Convers. Manag.* **2010**, *51*, 1449–1458. [[CrossRef](#)]
17. Kiss, P.; Jánosi, I.M. Comprehensive empirical analysis of ERA-40 surface wind speed distribution over Europe. *Energy Convers. Manag.* **2008**, *49*, 2142–2151. [[CrossRef](#)]
18. Seguro, J.V.; Lambert, T.W. Modern estimation of the parameters of the Weibull wind speed distribution for wind energy analysis. *J. Wind. Eng. Ind. Aerodyn.* **2000**, *85*, 75–84. [[CrossRef](#)]
19. Ülgen, K.; Hepbasli, A. Determination of Weibull parameters for wind energy analysis of Izmir, Turkey. *Int. J. Energy Res.* **2002**, *26*, 495–506. [[CrossRef](#)]
20. Chang, T.P. Performance comparison of six numerical methods in estimating Weibull parameters for wind energy application. *Appl. Energy* **2011**, *88*, 272–282. [[CrossRef](#)]
21. Available online: http://www.geonames.org/maps/google_39.25441_-76.70974.html (accessed on 15 July 2020).
22. National Renewable Energy Laboratory (NREL). Wind Research, Wind Resource Assessment. Available online: http://www.nrel.gov/wind/resource_assessment.html (accessed on 15 July 2020).
23. Hughes, W.K.; Williams, H.D.; Brenner, L.; Speakes-Backman, K. Ten-Year Plan (2012–2021) of Electric Companies in Maryland. Maryland Department of Natural Resources, 2013. Available online: <http://webapp.psc.state.md.us/intranet/Reports/TYP2021.pdf> (accessed on 15 July 2020).
24. U.S. Environmental Protection Agency. Ambient Air Monitoring Network Plan for Calendar Year 2017. Maryland Department of the Environment: Baltimore, MD, USA, 2016. Available online: <http://www.mde.state.md.us/programs/Air/AirQualityMonitoring/Documents/MDNetworkPlanCY2017.pdf> (accessed on 15 July 2020).
25. Emeis, S. *Wind Energy Meteorology: Atmospheric Physics for Wind Power Generation*; Springer: Berlin/Heidelberg, Germany, 2013; ISBN 978-3-642-30522-1.

26. Firtin, E.; Güler, Ö.; Akdağ, S.A. Investigation of wind shear coefficients and their effect on electrical energy generation. *Appl. Energy* **2011**, *88*, 4097–4105. [CrossRef]
27. Manwell, J.F.; McGowan, J.G.; Rogers, A.L. *Wind Energy Explained—Theory, Design, and Application*; John Wiley and Sons: Amherst, MA, USA, 2009; ISBN 0-471-49972-2.
28. Miller, S.T.K.; Keim, B.D.; Talbot, R.W.; Mao, H. Sea breeze: Structure, forecasting, and impacts. *Rev. Geophys.* **2003**, *41*, 1–31. [CrossRef]
29. Segal, M.; Avissar, R.; McCumber, M.C.; Pielke, R.A. Evaluation of Vegetation Effects on the Generation and Modification of Mesoscale Circulations. *J. Atmos. Sci.* **1988**, *45*, 2268–2293. [CrossRef]
30. Civerolo, K.L.; Sistla, G.; Rao, S.T.; Nowak, D.J. The effects of land use in meteorological modeling: Implications for assessment of future air quality scenarios. *Atmos. Environ.* **2000**, *34*, 1615–1621. [CrossRef]
31. Hoskins, B.J. Dynamical processes in the atmosphere and the use of models. *Q. J. R. Meteorol. Soc.* **1983**, *109*, 1–21. [CrossRef]
32. Cook, K.H.; Held, I.M. The Stationary Response to Large-Scale Orography in a General Circulation Model and a Linear Model. *J. Atmos. Sci.* **1992**, *49*, 525–539. [CrossRef]
33. Schär, C.; Smith, R.B. Shallow-Water Flow Past Isolated Topography. Part I: Vorticity Production and Wake Formation. *J. Atmos. Sci.* **1993**, *50*, 1373–1400. [CrossRef]
34. Grubišić, V.; Smith, R.B.; Schär, C. The Effect of Bottom Friction on Shallow-Water Flow Past an Isolated Obstacle. *J. Atmos. Sci.* **1995**, *52*, 1985–2005. [CrossRef]
35. Richter, I.; Mechoso, C.R. Orographic influences on the annual cycle of Namibian stratocumulus clouds. *Geophys. Res. Lett.* **2004**, *31*, 1–4. [CrossRef]
36. Buermann, W.; Dong, J.; Zeng, X.; Myneni, R.B.; Dickinson, R.E. Evaluation of the Utility of Satellite-Based Vegetation Leaf Area Index Data for Climate Simulations. *J. Clim.* **2001**, *14*, 3536–3550. [CrossRef]
37. Seaman, L.N. Meteorological modeling for air-quality assessments. *Atmos. Environ.* **2000**, *34*, 2231–2259. [CrossRef]
38. Klink, K. Trends in mean monthly maximum and minimum surface wind speeds in the coterminous United States, 1961 to 1990. *Clim. Res.* **1999**, *13*, 193–205. [CrossRef]
39. Balling, R.C., Jr.; Cerverny, R.S. Long-Term Associations between Wind Speeds and the Urban Heat Island of Phoenix, Arizona. *J. Clim. Appl. Meteorol.* **1987**, *26*, 712–716. [CrossRef]
40. Bornstein, R.D.; Johnson, D.S. Urban-rural wind velocity differences. *Atmos. Environ.* **1977**, *11*, 597–604. [CrossRef]
41. Lee, D. The influence of atmospheric stability and the urban heat island on urban-rural wind speed differences. *Atmos. Environ.* **1979**, *13*, 1175–1180. [CrossRef]
42. Stauffer, R.M.; Thompson, A.M. Bay breeze climatology at two sites along the Chesapeake bay from 1986–2010: Implications for surface ozone. *J. Atmos. Chem.* **2013**, *72*, 355–372. [CrossRef]
43. Loughner, C.P.; Allen, D.J.; Pickering, K.E.; Zhang, D.-L.; Shou, Y.-X.; Dickerson, R.R. Impact of fair-weather cumulus clouds and the Chesapeake Bay breeze on pollutant transport and transformation. *Atmos. Environ.* **2011**, *45*, 4060–4072. [CrossRef]
44. Martins, D.K.; Stauffer, R.M.; Thompson, A.M.; Halliday, H.S.; Kollonige, D.W.; Joseph, E.; Weinheimer, A.J. Ozone correlations between mid-tropospheric partial columns and the near-surface at two mid-Atlantic sites during the DISCOVER-AQ campaign in July 2011. *J. Atmos. Chem.* **2013**, *72*, 373–391. [CrossRef] [PubMed]
45. Irwin, J.S. A theoretical variation of the wind profile power-law exponent as a function of surface roughness and stability. *Atmos. Environ.* **1979**, *13*, 191–194. [CrossRef]
46. Bailey, H.; McDonald, L. *Wind Resource Assessment Handbook*; AWS Scientific Inc: Albany, NY, USA, 1997.
47. Johnson, G.L. *Wind Energy Systems*. Electronic Edition. 2006. Available online: http://www.pssurvival.com/ps/windmills/Wind_Energy_Systems_Johnson_2001.pdf (accessed on 15 July 2020).
48. Mohammadi, K.; Alavi, O.; Mostafaeipour, A.; Goudarzi, N.; Jalilvand, M. Assessing different parameters estimation methods of Weibull distribution to compute wind power density. *Energy Convers. Manag.* **2016**, *108*, 322–335. [CrossRef]
49. Justus, C.G. *Winds and Wind System Performance*; Franklin Institute Press: Philadelphia, PA, USA, 1978.
50. IEC. *International Standard IEC 61400-1: Wind Turbines—Part 1: Design Requirements*; International Electrotechnical Commission: Geneva, Switzerland, 2005.
51. Elliot, D.L.; Schwartz, M.N. *Wind Energy Potential in the United States, PNL-SA-23109*; Pacific Northwest Laboratory: Richmond, WA, USA, 1993; NTIS No. DE94001667.

52. Mohammadi, K.; Mostafaeipour, A.; Sedaghat, A.; Shamshirband, S.; Petković, D. Application and economic viability of wind turbine installation in Lutak, Iran. *Environ. Earth Sci.* **2016**, *75*, 1–16. [[CrossRef](#)]
53. Christiner, M.; Dobbins, R.; Ndegwa, A.; Sivak, J. Rooftop Wind Turbine Feasibility in Boston, Massachusetts. Master's Thesis, Worcester Polytechnic Institute, Worcester, MA, USA, 2010.
54. Singh, R.K.; Ahmed, M.R. Blade design and performance testing of a small wind turbine rotor for low wind speed applications. *Renew. Energy* **2013**, *50*, 812–819. [[CrossRef](#)]
55. Kishore, R.A.; Coudron, T.; Priya, S. Small-scale wind energy portable turbine (SWEPT). *J. Wind. Eng. Ind. Aerodyn.* **2013**, *116*, 21–31. [[CrossRef](#)]
56. Goudarzi, N.; Zhu, W.D.; Bahari, H. Numerical simulation of a fluid flow inside a novel ducted wind turbine. In Proceedings of the ASME 4th Joint US-European Fluids Engineering Division Summer Meeting, Chicago, IL, USA, 3–7 August 2014.
57. Catalogue of European Urban Wind Turbine Manufacturers. Available online: http://www.urbanwind.net/pdf/Catalogue_Final.pdf (accessed on 15 July 2020).
58. Bakhshi, R.; Sandborn, P.A. A Return on Investment Model for the Implementation of New Technologies on Wind Turbines. *IEEE Trans. Sustain. Energy* **2017**, *9*, 284–292. [[CrossRef](#)]
59. Bruck, M.; Sandborn, P.; Goudarzi, N. A Levelized Cost of Energy (LCOE) model for wind farms that include Power Purchase Agreements (PPAs). *Renew. Energy* **2018**, *122*, 131–139. [[CrossRef](#)]
60. EIA. Electric Power Monthly. Available online: https://www.eia.gov/electricity/monthly/epm_table_grapher.php?t=epmt_5_6_a. (accessed on 15 July 2020).
61. Bahariaenergy. Available online: <https://www.bahariaenergy.com/> (accessed on 15 July 2020).

Publisher's Note: MDPI stays neutral with regard to jurisdictional claims in published maps and institutional affiliations.



© 2020 by the authors. Licensee MDPI, Basel, Switzerland. This article is an open access article distributed under the terms and conditions of the Creative Commons Attribution (CC BY) license (<http://creativecommons.org/licenses/by/4.0/>).